

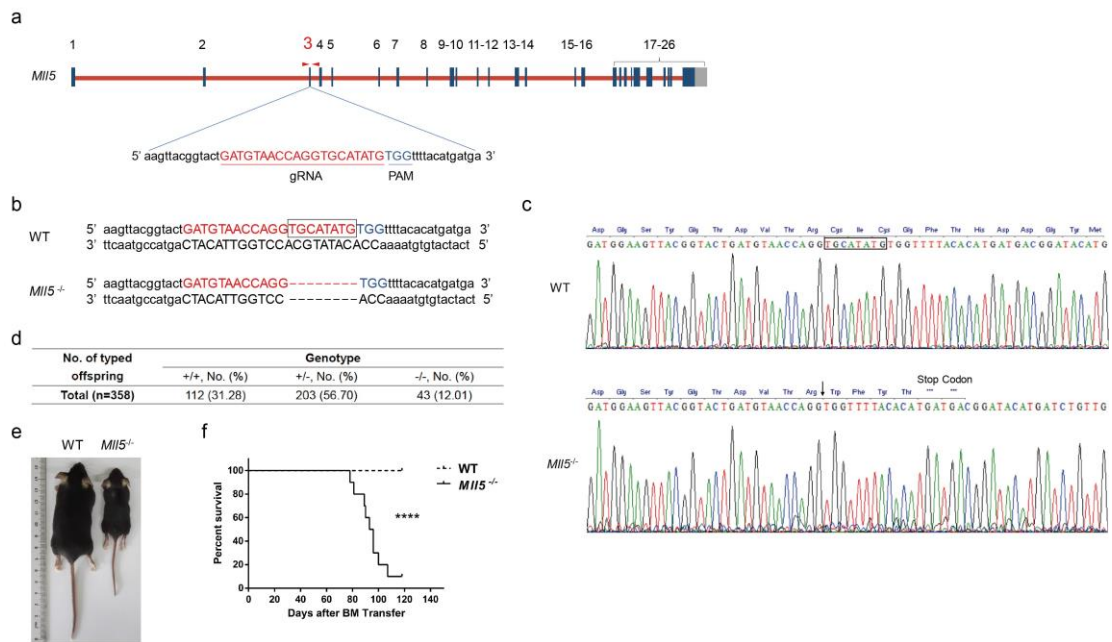
1 **MLL5 suppresses antiviral innate immune response by facilitating**

2 **STUB1-mediated RIG-I degradation**

3

4 Zhou et al.

5



6

7 **Supplementary Figure 1. Generation of *Mli5*-deficient mice with CRISPR-Cas9**

8 approach. **(a)** Graphic representation of strategy used to generate *Mli5*^{-/-} mice. gRNA

9 (red) and PAM (blue) sequences locus in exon 3 of *Mli5* gene. **(b)** DNA sequence of

10 WT (upper) and *Mli5*^{-/-} mice (bottom). The region of the target sequence is shown in

11 red. The black box indicates the nucleotides lost in *Mli5*^{-/-} mice. **(c)** Sequence analysis

12 of the the Reverse Transcription-PCR band in MEFs from WT (upper) and *Mli5*^{-/-}

13 mice (bottom). The nucleotide sequence confirms the reading frame shift in exon 3 in

14 *Mli5*^{-/-} mice; a premature stop codon (TGA) in exon 3 is induced. **(d)** Number and

15 frequency of WT, *Mli5*^{+/-} and *Mli5*^{-/-} pups by *Mli5*^{+/-} intercrosses at the time of

16 weaning. **(e)** Postnatal growth retardation in *Mli5*-deficient mice; one pair of 6-week-

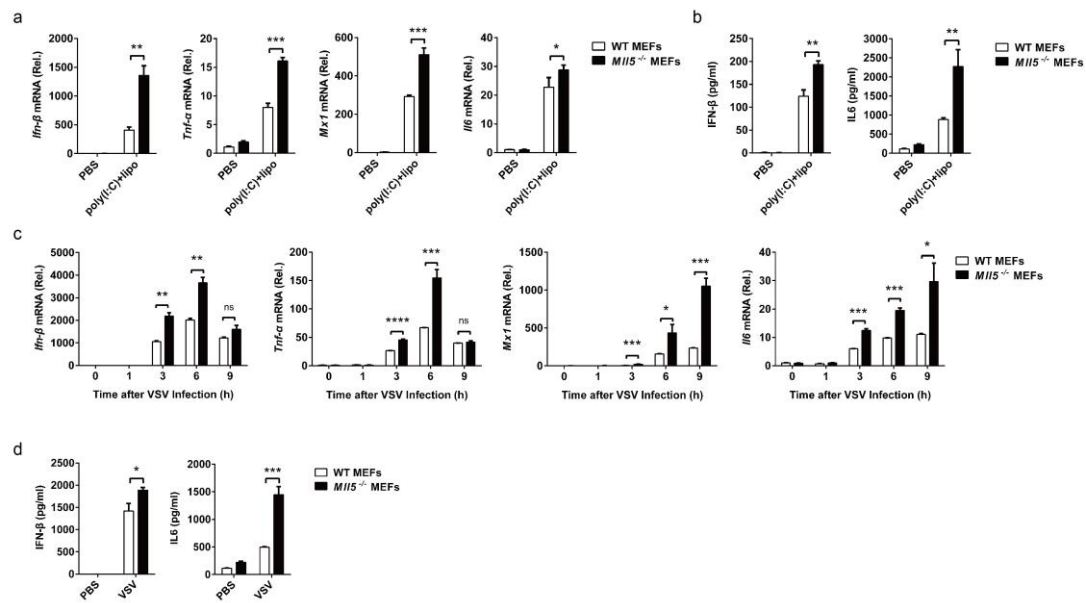
17 old WT and *Mli5*^{-/-} male littermates. **(f)** Survival curves of lethally irradiated

18 recipients transplanted with WT and *Mli5*^{-/-} BM (n=10). Data were analyzed by log-

19 rank (Mantel-Cox) test. (**** p<0.0001).

20

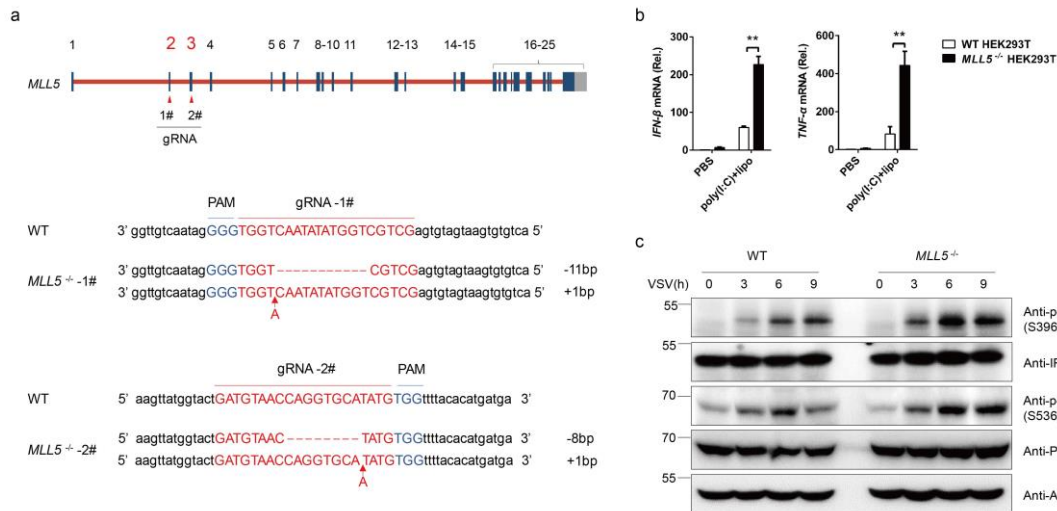
21



22

23 **Supplementary Figure 2.** MLL5 selectively suppresses RLR-mediated antiviral
 24 innate immune response in mouse embryonic fibroblasts. **(a)** Expression of *Ifn-β*,
 25 *Tnf-α*, *Mx1* and *Il6* mRNA in MEFs from WT or *Mll5*^{-/-} mice stimulated with
 26 intracellular poly(I:C) (1 μg/ml) for 6 h. *Gapdh* served as a control. **(b)** ELISA
 27 quantification of IFN-β and IL-6 secretion in MEFs treated as in **a**. **(c)** Expression of
 28 *Ifn-β*, *Tnf-α*, *Mx1* and *Il6* mRNA in MEFs from WT or *Mll5*^{-/-} mice infected with
 29 VSV-GFP (MOI:1) . *Gapdh* served as a control. **(d)** ELISA quantification of IFN-β
 30 and IL-6 secretion in MEFs from WT or *Mll5*^{-/-} mice infected with VSV-GFP
 31 (MOI:1) for 6 h. Data were from three independent experiments and were analyzed
 32 with the Student's *t*-test (two-tailed) and were presented as mean ± SD. (* *p*<0.05,
 33 ** *p*<0.01, *** *p*<0.001, **** *p*<0.0001).

34

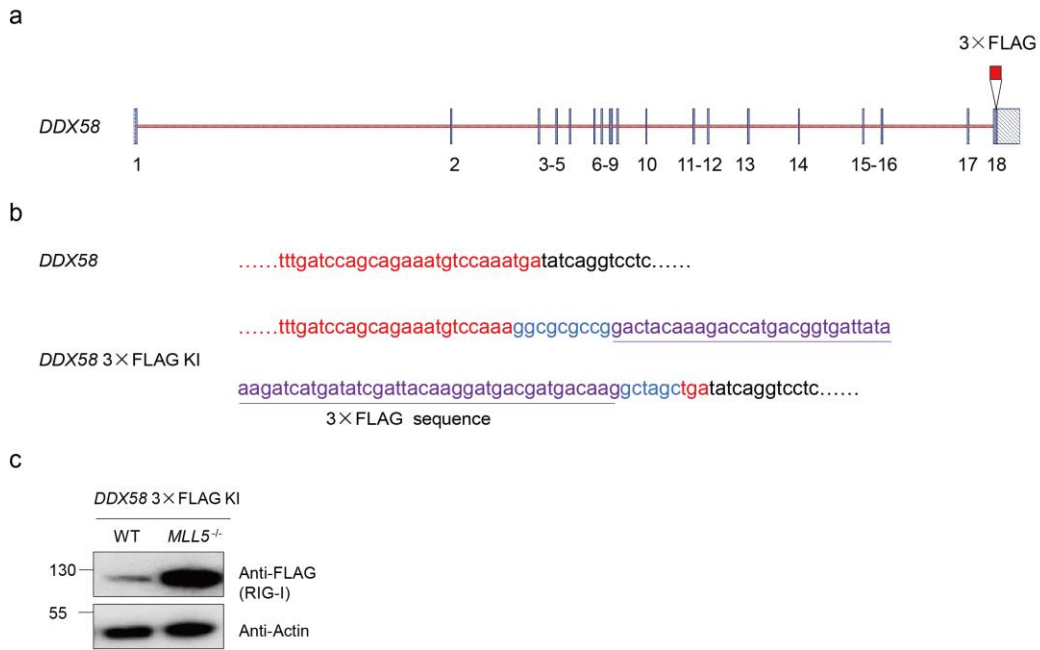


35

36 **Supplementary Figure 3.** MLL5 suppresses RLR-mediated immune response in
 37 HEK293T cells. **(a)** Graphic representation of strategy used to generate *MLL5*^{-/-}
 38 HEK293T cells (upper) and DNA sequence of *MLL5*^{-/-} HEK293T cells (bottom).
 39 gRNA (red) and PAM (blue) sequences locus in exon 2 and 3 of *MLL5* gene. The
 40 column on the right indicates the number of inserted or deleted bases. **(b)** Expression
 41 of *IFN-β* and *TNF-α* mRNA in WT and *MLL5*^{-/-} (2#) HEK293T cells stimulated with
 42 intracellular poly(I:C) (1 μg/ml) for 6 h. *GAPDH* served as a control. **(c)** Immunoblot
 43 analysis of p-IRF3 and P65 in WT and *MLL5*^{-/-} (2#) HEK293T cells upon infection
 44 with VSV-GFP (MOI:1) for indicated times. Actin served as a loading control. Data
 45 were representative of three independent experiments with similar results **(c)** or were
 46 from three independent experiments **(b)** and were analyzed with the Student's *t*-test
 47 (two-tailed) and were presented as mean ± SD. (** p < 0.01).

48

49

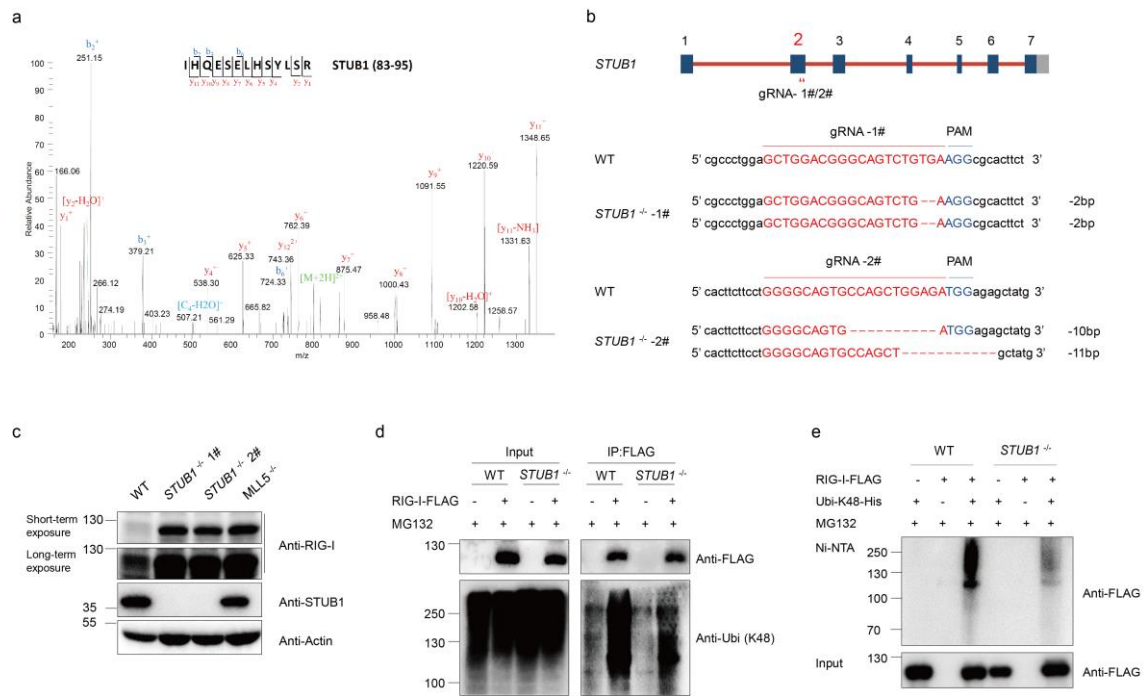


50

51 **Supplementary Figure 4.** Generation of FLAG-tagged endogenous RIG-I protein in
 52 HEK293T cells. **(a)** Schematic of 3xFLAG coding sequence insertion in *DDX58*
 53 gene in WT and *MLL5*^{-/-} HEK293T cells. **(b)** DNA sequence around the stop codon
 54 (tga, red letters) of *DDX58* gene in WT cells (upper) and the 3xFLAG knock-in cells
 55 (bottom). Purple indicates the 66-bps 3xFLAG coding sequence. Red indicates the
 56 coding sequence of *DDX58*. Blue indicates the restriction enzyme cutting sites. **(c)**
 57 Immunoblot analysis of FLAG-tagged RIG-I in the *DDX58* 3xFLAG knock-in WT
 58 and *MLL5*^{-/-} HEK293T cells. Actin served as a loading control. Data are representative
 59 of three independent experiments with similar results.

60

61



62

63 **Supplementary Figure 5.** Identification of STUB1 as the E3 ligase of RIG-I. **(a)**

64 STUB1 in RIG-I-interacting proteins identified by mass spectrometry. **(b)** Graphic

65 representation of strategy used to generate *STUB1*^{-/-} HEK293T cells (upper) and DNA

66 sequence of *STUB1*^{-/-} HEK293T cells (bottom). gRNA (red) and PAM (blue)

67 sequences locus in exon 2 of *STUB1* gene. The column on the right indicates the

68 number of inserted or deleted bases. **(c)** Immunoblot analysis of RIG-I and STUB1 in

69 the WT and *STUB1*^{-/-} HEK293T cells. Actin served as a loading control. **(d)** Co-

70 immunoprecipitation and immunoblot analysis of K48-linked polyubiquitination of

71 RIG-I in WT and *STUB1*^{-/-} (1#) HEK293T cells transfected with RIG-I-FLAG and

72 treated with MG132 (5 μM) for 12 h before. **(e)** His-pull down and immunoblot

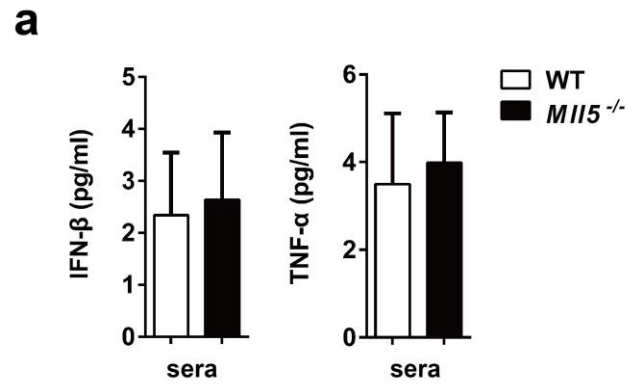
73 analysis of K48-linked polyubiquitination of RIG-I in WT and *STUB1*^{-/-} (1#)

74 HEK293T cells cotransfected with RIG-I-FLAG and mutant ubiquitin K48-ubi-His

75 and treated with MG132 (5 μM) for 12 h. Data are representative of three independent

76 experiments with similar results.

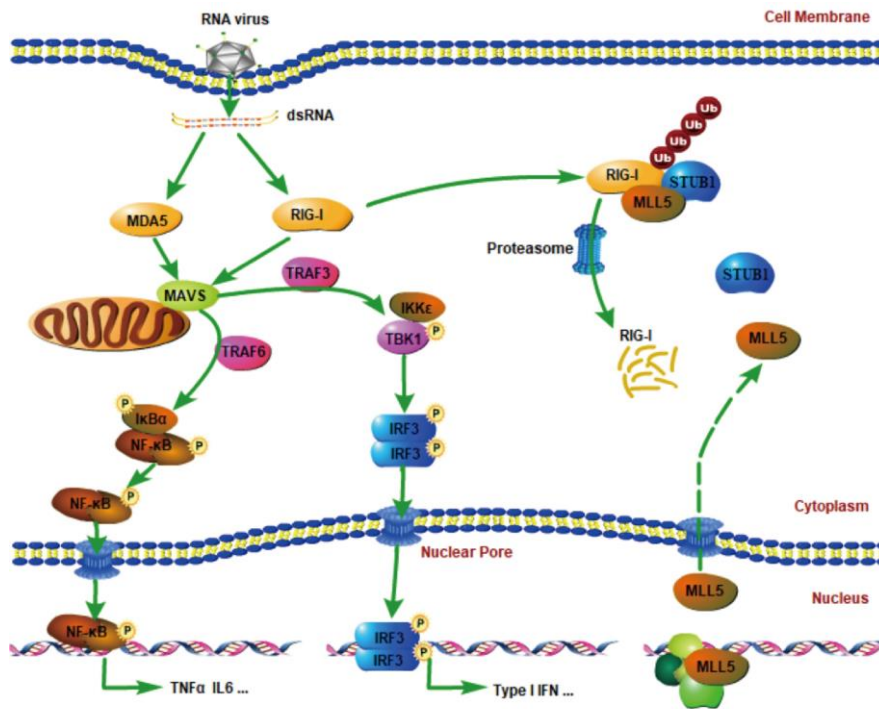
77



78

79 **Supplementary Figure 6.** ELISA quantification of IFN-β and TNF-α in sera in 6-9
80 weeks old WT or *MI15*^{-/-} littermates (n=3).

81

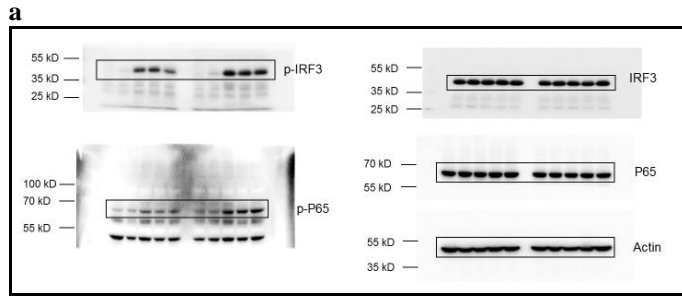


82

83 **Supplementary Figure 7.** Working model. A small fraction of MLL5 proteins
 84 located in the cytoplasm facilitated interaction between RIG-I and its E3 ligase
 85 STUB1 and promoted K48-linked polyubiquitination and proteasome degradation of
 86 RIG-I. MLL5 translocate from the nucleus to the cytoplasm in responses to RNA
 87 virus infection, thereby promoting degradation of RIG-I through E3 ubiquitin ligase
 88 STUB1.

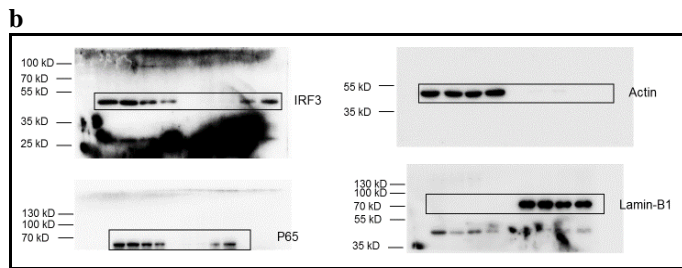
89

90



91

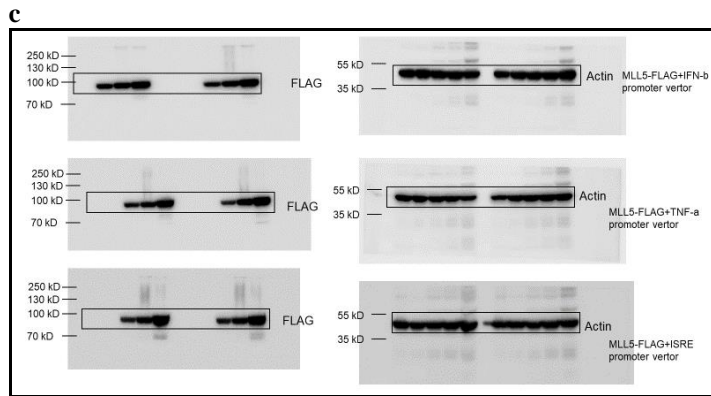
92



93

94

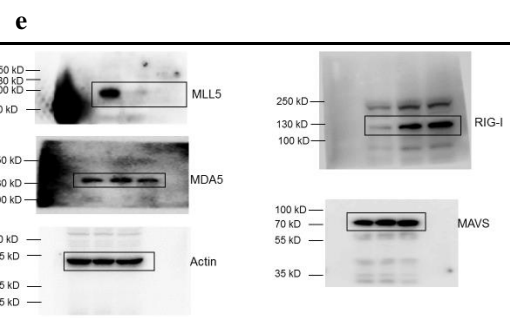
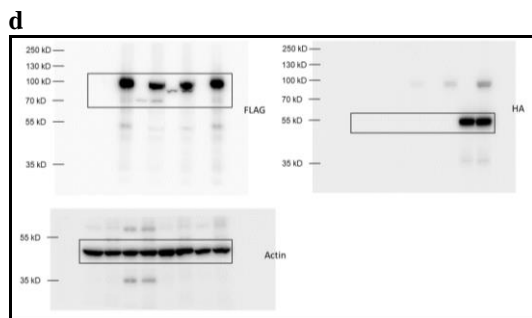
95



96

97

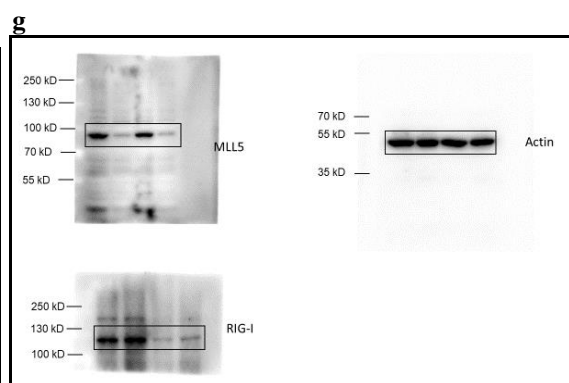
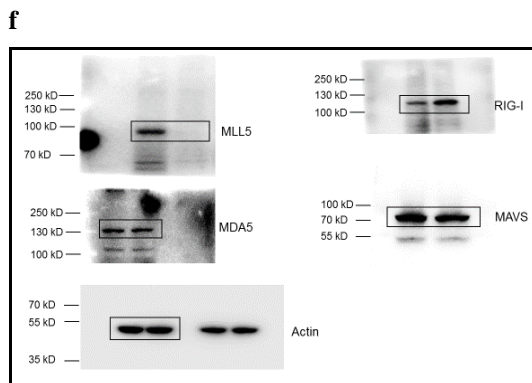
98



99

100

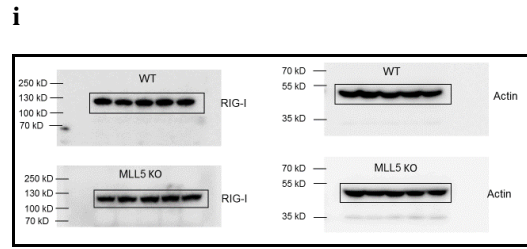
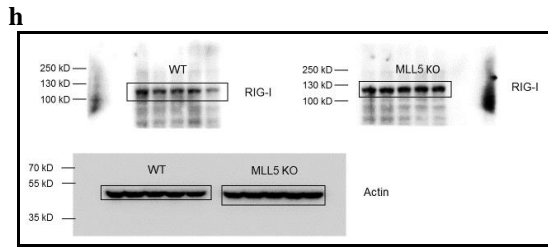
101



102

103

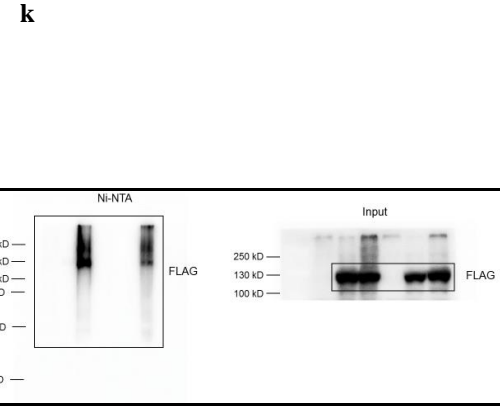
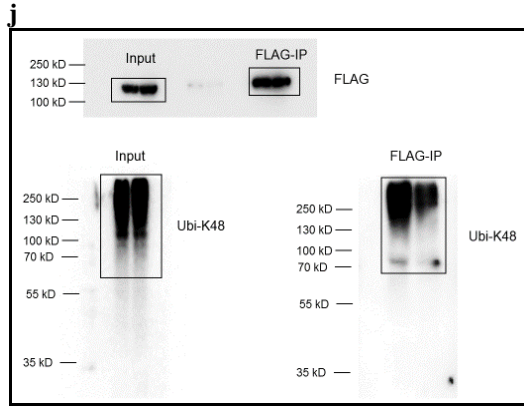
104



105

106

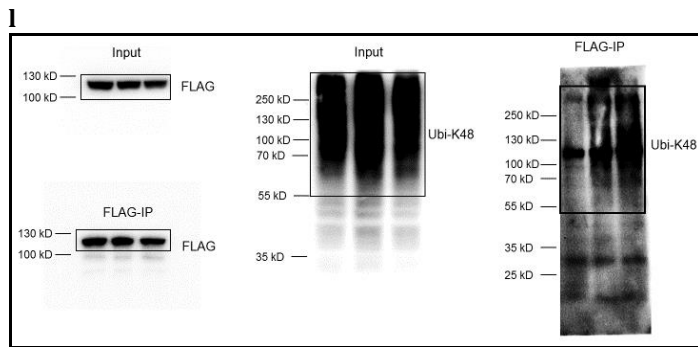
107



108

109

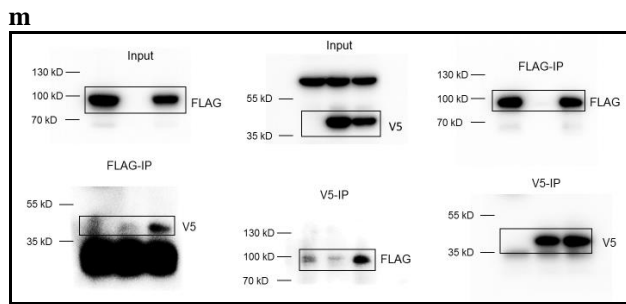
110



111

112

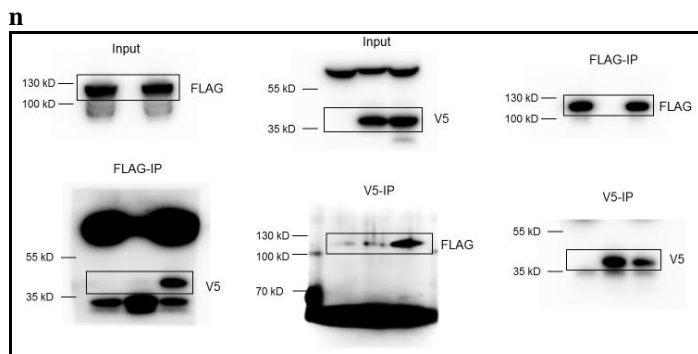
113



114

115

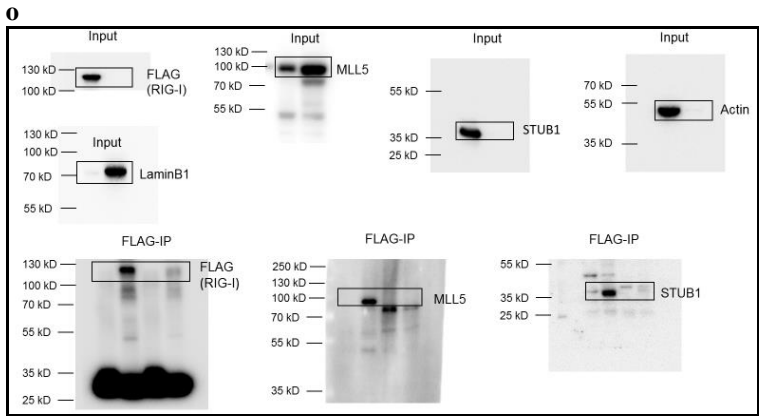
116



117

118

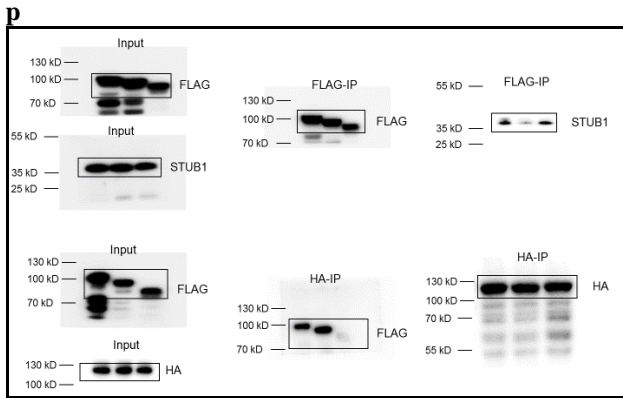
119



120

121

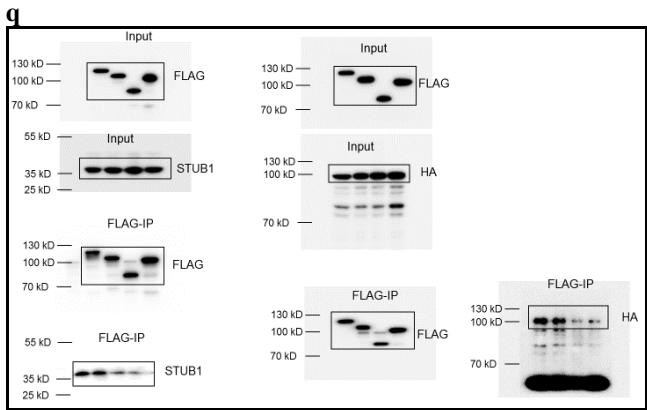
122



123

124

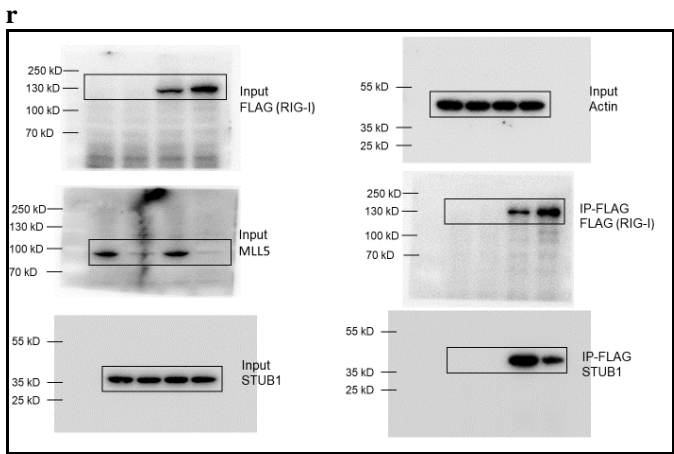
125



126

127

128

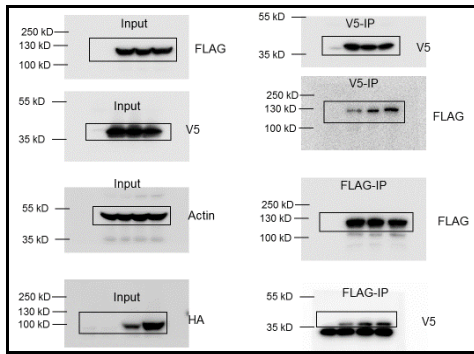


129

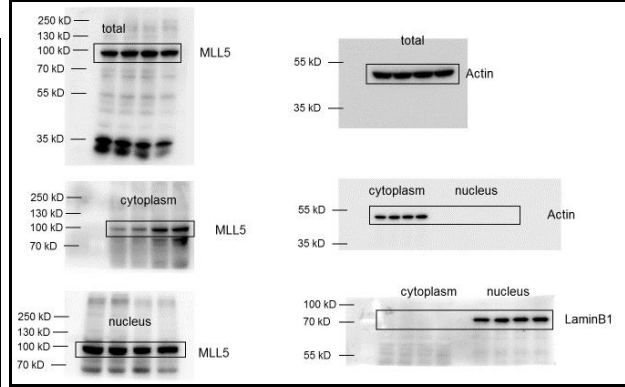
130

131

s



t

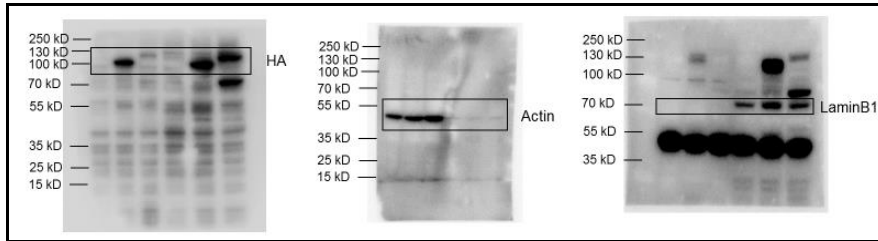


132

133

134

u

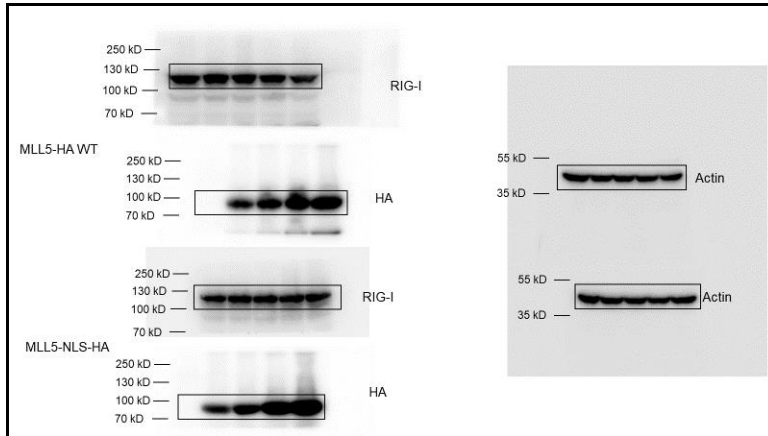


135

136

137

v

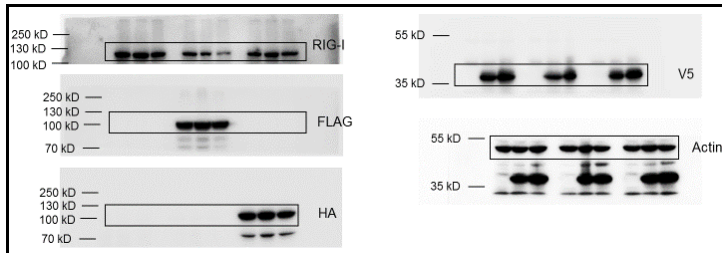


138

139

140

w



141

142

143

144

145

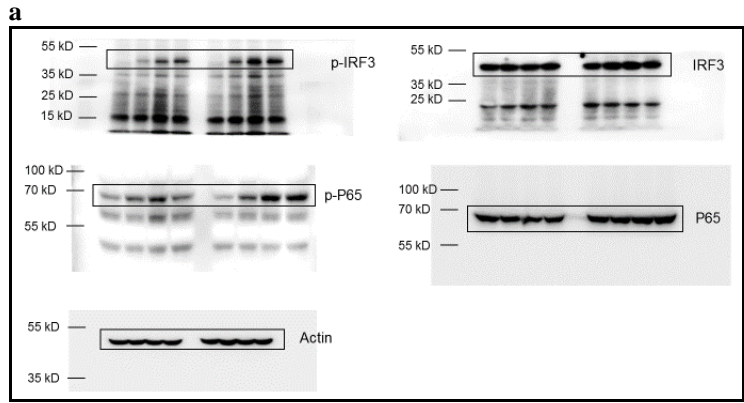
146

147

148

Supplementary Figure 8. Uncropped dcans of the western blots related to main figures. (a-c) related to Figure 2 a-c, (d-g) related to Figure 4 a-d, (h-l) related to Figure 4 g-k, (m-o) related to Figure 5 a-c, (p-q) related to Figure 5 e and f, (r-s) related to Figure 6 a and b, (t-w) related to Figure 7 a, c, e and f.

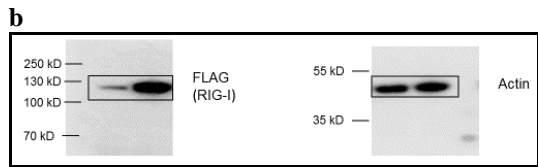
149



150

151

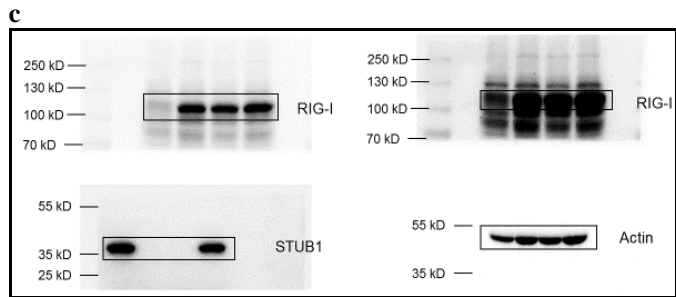
152



153

154

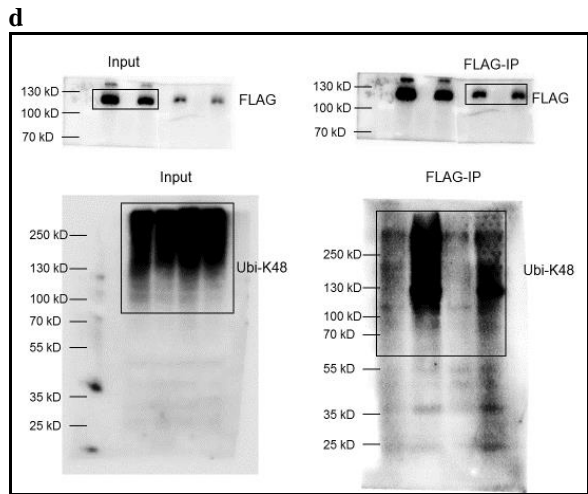
155



156

157

158



159

160

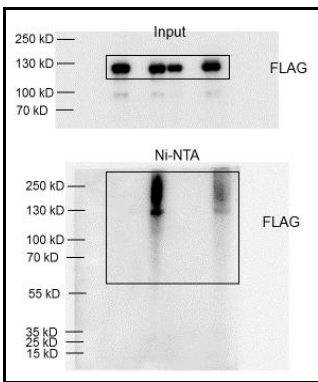
161

162

163

164

e



Supplementary Figure 9. Uncropped dcans of the western blots related to Supplementary Figures. **(a)** related to Supplementary Figure 3 c, **(b)** related to Supplementary Figure 4 c, **(c-e)** related to Supplementary Figure 5 d-f.

165 **Supplementary Table 1.** Relative band densities indicating RIG-I protein levels in
166 WT and *MLL5*^{-/-} HEK293T cells treated with CHX (100 µg/ml).

Time	0h	15h	20h	25h	30h
WT	1.0	0.90	0.68	0.69	0.60
<i>MLL5</i> ^{-/-}	1.0	0.98	1.02	1.05	1.0
Time	0h	6h	12h	18h	24h
WT	1.0	0.95	0.68	0.48	0.47
<i>MLL5</i> ^{-/-}	1.0	1.02	0.94	0.86	0.88

167 Actin served as a loading control. Band density indicating protein amount was
168 quantified using Image J software.

169

170 **Supplementary Table 2.** Candidates RIG-I-interacting proteins identified by mass
171 spectrometry.

seq count	gene name
703	DDX58
91	HUWE1
34	MLL5
41	TRIM28
40	HECTD1
29	HERC5
25	RNF135
20	TRIM21
13	TRIM25
9	UBR5
7	ECM29
6	MUL1
4	HUWE1
3	RNF138
4	HERC1
4	STUB1
3	MARCH7
3	XIAP
3	UBL4A
3	UFL1
2	KCMF1
2	DTX3L
2	RNF187
2	TRIM26
2	RANBP2
2	CBX4

172

173

174 **Supplementary Table 3.** Relative band densities indicating MLL5 protein levels in
175 the nuclear and cytoplasmic fractions in WT HEK293T cells infected with VSV-GFP
176 (MOI:1).

Time (VSV-GFP)	0h	5h	10h	15h
Cytoplasm	1.0	1.19	1.65	1.70
Nucleus	1.0	0.96	0.83	0.85
Time (VSV-GFP)	0h	4h	8h	
Cytoplasm	1.0	1.10	1.62	
Nucleus	1.0	0.95	0.87	

177 Actin served as a cytoplasmic control. Lamin B1 served as a nuclear protein control.

178 Band density indicating protein amount was quantified using Image J software.

179

180

181 **Supplementary Table 4.** Relative band densities indicating RIG-I protein levels in
182 *MLL5*^{-/-} HEK293T cells transfected with different amount of MLL5-HA or MLL5-
183 NLS-HA plasmids (0, 300, 600, 1000 and 2000 ng).

Amount of Plasmids	0	300ng	600ng	1000ng	2000ng
MLL5-HA	1.0	0.46	0.46	0.49	0.37
	1.0	0.85	0.80	0.76	0.75
MLL5-HA-NLS	1.0	1.22	1.16	1.02	0.93
	1.0	1.04	1.08	1.02	1.0

184 Actin served as a loading control. Band density indicating protein amount was
185 quantified using Image J software.